

# 2D/3D Image fusion for accurate target localization and evaluation of a mask based stereotactic system in fractionated stereotactic radiotherapy of cranial lesions

Jian-Yue Jin,<sup>a)</sup> Samuel Ryu, Kathleen Faber, Tom Mikkelsen, Qing Chen, Shidong Li, and Benjamin Movsas

Department of Radiation Oncology, Henry Ford Hospital, 2799 W. Grand Boulevard, Detroit, Michigan 48202

(Received 5 June 2006; revised 17 October 2006; accepted for publication 19 October 2006; published 16 November 2006)

The purpose of this study was to evaluate the accuracy of a two-dimensional (2D) to three-dimensional (3D) image-fusion-guided target localization system and a mask based stereotactic system for fractionated stereotactic radiotherapy (FSRT) of cranial lesions. A commercial x-ray image guidance system originally developed for extracranial radiosurgery was used for FSRT of cranial lesions. The localization accuracy was quantitatively evaluated with an anthropomorphic head phantom implanted with eight small radiopaque markers (BBs) in different locations. The accuracy and its clinical reliability were also qualitatively evaluated for a total of 127 fractions in 12 patients with both kV x-ray images and MV portal films. The image-guided system was then used as a standard to evaluate the overall uncertainty and reproducibility of the head mask based stereotactic system in these patients. The phantom study demonstrated that the maximal random error of the image-guided target localization was  $\pm 0.6$  mm in each direction in terms of the 95% confidence interval (CI). The systematic error varied with measurement methods. It was approximately 0.4 mm, mainly in the longitudinal direction, for the kV x-ray method. There was a 0.5 mm systematic difference, primarily in the lateral direction, between the kV x-ray and the MV portal methods. The patient study suggested that the accuracy of the image-guided system in patients was comparable to that in the phantom. The overall uncertainty of the mask system was  $\pm 4$  mm, and the reproducibility was  $\pm 2.9$  mm in terms of 95% CI. The study demonstrated that the image guidance system provides accurate and precise target positioning. © 2006 American Association of Physicists in Medicine. [DOI: 10.1118/1.2392605]

Key words: fractionated stereotactic radiotherapy, image guidance, thermal plastic mask fixation, position accuracy, image fusion

## I. INTRODUCTION

Fractionated stereotactic radiotherapy (FSRT) has radiobiologic benefits over single-fraction stereotactic radiosurgery (SRS) for a variety of intracranial applications, especially for large lesions and lesions located in eloquent regions of the brain.<sup>1-3</sup> For both FSRT and SRS, effective immobilization and localization of the target are crucial. Usually invasive stereotactic frame systems such as the Brown-Robert-Wells frame are used for single-fraction SRS. In such systems, invasive screws are fixed onto the patient's skull for immobilization and fiducial bars on the position frame are used to localize the target. Submillimeter accuracy is usually achieved.

However, such systems are not suitable for FSRT. Consequently, different immobilization and localization methods have been developed for FSRT applications. They can be categorized into the following groups: (1) Relocatable invasive systems such as the ATLON system;<sup>4</sup> (2) relocatable noninvasive frame systems based on fixation of maxillary/external auditory canals;<sup>5-8</sup> (3) thermal plastic or vacuum

formed mask fixation;<sup>9,10</sup> (4) external image or sensor guided optical localization systems,<sup>11,12</sup> and (5) internal bony anatomy or implanted marker based x-ray image guided localization systems.<sup>13,14</sup>

The thermal plastic mask based head immobilization system has gained wide acceptance due to its easy use, relative comfort for patients, and acceptable localization accuracy and reproducibility. The Novalis Shaped Beam Radiosurgery unit employs the thermal plastic mask based stereotactic localization system for the intracranial FSRT application.

However, a recent study showed that the localization accuracy and reproducibility of this system was not ideal, with a maximal deviation up to 7 mm in a single direction.<sup>15</sup> The accuracy reported by this study was considerably poorer than the results reported by other researchers.<sup>16-18</sup> Nevertheless, this limited accuracy is understandable considering the following intrinsic properties of the thermal plastic mask: (1) the thermal plastic mask shrinks slightly after cooling down; consequently, 1-4 mm spacers are often added to fit the patient comfortably into the mask during treatment. (2) The material is slightly elastic so that patients could move their heads slightly within the mask, especially in the longitudinal

(superior/inferior) and rotational directions. (3) Many steps in the localization procedure require extensive technical attention.

The Novalis Shaped Beam Radiosurgery unit also uses an x-ray image-guided system in target localization for extracranial radiosurgery. The initial version of the image guidance system used a three-degrees (3D) of freedom fusion technique, referred to as “3D fusion,” which automatically fuses two two-dimensional (2D) localization x-ray images with two corresponding digital reconstructed radiographs (DRRs) with fixed angles. The accuracy of such an image guidance system was limited due to potential rotational errors in patient setup. Recently, a six-degrees (6D) of freedom fusion technique, referred to as “6D fusion,” was developed to improve the localization accuracy. Unlike the “3D fusion” technique, it fuses the 2D localization x-ray images directly with the three-dimensional (3D) computed tomography (CT) simulation images in six degrees of freedom. Specifically, the software compares the two x-ray images with corresponding DRRs calculated from the CT images with various rotational and translational shifts and finds the pair of DRRs with maximal similarity to the x-ray images to be the best match. A phantom study demonstrated that the “6D fusion” method improved the localization accuracy compared with 3D fusion when rotational deviation existed.<sup>19</sup> The “6D fusion” is formally known as the 2D/3D image registration technique, while the “3D fusion” is rather a 2D/2D image registration technique. We have developed a clinical procedure to integrate this “6D fusion” technique into the mask based stereotactic system for intracranial FSRT applications. This article describes the details of this procedure and evaluates its localization accuracy and reliability. In addition, as a by-product, the “6D fusion” technique is also used as a standard to systematically evaluate the positioning accuracy and reproducibility of the thermal plastic mask based stereotactic localization system.

## II. MATERIAL AND METHODS

### A. 2D/3D image fusion guided procedure for intracranial FSRT

Unlike the image-guided procedure for extracranial radiosurgery, which utilizes the infrared based ExacTrac body marker system to initially setup patients, this procedure uses the thermal plastic head mask based stereotactic localization system (a templated localization box) and room lasers for initial patient setup. The image-guided system is employed to further improve the localization accuracy. At the same time, it also provides a measure to evaluate the accuracy of the mask system. This section describes the details of the mask and the image guided systems, and the patient procedure that requires an integration of the two systems.

#### 1. Mask based stereotactic localization system

The head mask consists of three main components: a rear mask to conform to the posterior contour of the patient’s head, a middle mask with two strong strips to fix the maxil-

lary region and the forehead, and a large top mask to conform to the patient’s facial contour. In addition, a firm fit mold is added over the nasal bridge to minimize head rotation, as well as a dental support strip to prevent longitudinal movement. All three mask pieces are jointly attached to a U-shaped frame with clips. Spacer bars with 1–4 mm thickness can be added to adjust the pressure in case the mask shrinks, or the patient head size changes due to facial swelling (for example, after taking steroids), or due to weight loss. A CT stereotactic localization box is attached to the U-shaped frame during CT simulation. Three sets of fiducial bars in the localization box are reconstructed in the treatment planning system (BrainScan 3.5, Brainlab AG, Heimstetten, Germany) from the CT images. The target position relative to the localization box coordinates is then established. After the planning process is completed, the isocenter position (depicted as a fine cross) is printed onto the Target Positioner sheets. The template sheets are then attached to the corresponding faces of the Target Positioner Box according to redundant matching marks. During patient setup, the Positioner Box is attached to the U-shaped frame and the patient is set up with room lasers aligned with the isocenter crosses at the Positioner sheets.

#### 2. X-ray image-guided localization system

The x-ray image-guided system, namely, the ExacTrac/Novalis Body system (Version 3.5, BrainLab, AG, Heimstetten, Germany) was initially developed for extracranial radiosurgery applications. It is an integration of an infrared ExacTrac component and an x-ray imaging component. The ExacTrac component consists of two infrared cameras mounted on the ceiling of the treatment room, monitoring patient position according to infrared reflective markers placed on the patient’s skin. The infrared cameras can identify each marker’s position with a precision better than 0.3 mm.<sup>20</sup>

The x-ray imaging component consists of two floor-mounted kV x-ray tubes, projecting obliquely from lateral to medial, posterior to anterior and superior to inferior onto two corresponding flat panel detectors suspended from the ceiling, with the patient in the supine position with head toward the gantry. The centerlines from the two tubes form a 62° angle at the linac isocenter. The oblique plane defined by the two centerlines has an approximately 53° angle to the horizontal plane as shown in Fig. 1. Two x-ray images are acquired after the patient’s initial setup. The ExacTrac/Novalis software then registers these two images with the patient’s 3D CT simulation images. The software provides manual matching, “3D fusion,” “6D fusion” and “implanted marker matching” options for registration of the images. After image registration, the software provides three translational deviations for correcting the setup position. Three rotational deviations are also provided for 6D fusion. Then, the patient position is precisely adjusted by automatically or manually translating the couch guided by the integrated ExacTrac system.

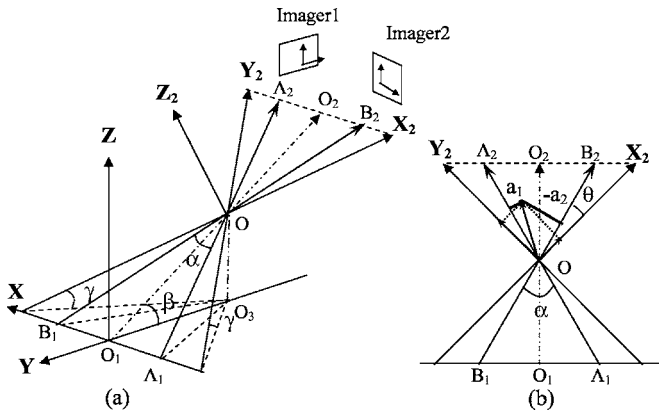


FIG. 1. (a) Illustration of the configuration of the Novalis x-ray system, and the transformation of the deviation measured in two x-ray images into the deviation in the patient coordinate system. (b) Detail in the imaging plane.

### 3. Patient procedure

The patient was immobilized with the BrainLab mask system and CT scanned with the stereotactic localization box attached. The isocenter was defined. The CT images and the isocenter were imported to the BrainScan treatment planning system. The treatment planning procedure was exactly the same as the standard procedure for the mask based stereotactic localization method, except the plan geometry and CT images were exported to the ExacTrac/Novalis system control computer at the treatment console. The patient was initially set up with the stereotactic positioner box for each fraction. At this point, a reference star with four infrared reflective markers was attached to the treatment couch. The ExacTrac system read the initial patient position and continuously monitored the position through the reference star. Two localization images were then acquired. The auto “6D fusion” was performed and the matching of the bony structures between the DRRs and the images was reviewed. The patient’s position was readjusted by couch translations, guided by the ExacTrac system, according to the fusion results. The image-guided system was also used as a quick quality assurance (QA) check tool. If the “6D fusion” suggested an unusual deviation (for example, the deviation was larger than 5 mm or three degrees), extra care would be taken to check the setup and mask immobilization of the patient. Anterior to Posterior (AP) and lateral MV portal films were also taken for the first fraction and after every 5–6 fractions. It should be pointed out that in this study, only the three translational dimensions were adjustable (a 6D adjustable table will be installed in the future). The readjustment moved the patient to the correct isocenter position, but did not correct the rotational deviations. It should also be pointed out that if the isocenter was in the inferior portion of the cranium, the mandible in the image would be excluded during the “6D fusion.”

### B. Evaluation of the “6D-fusion” image-guided system

The human skull is a rigid structure that can be well represented by an anthropomorphic head phantom. A quantitative

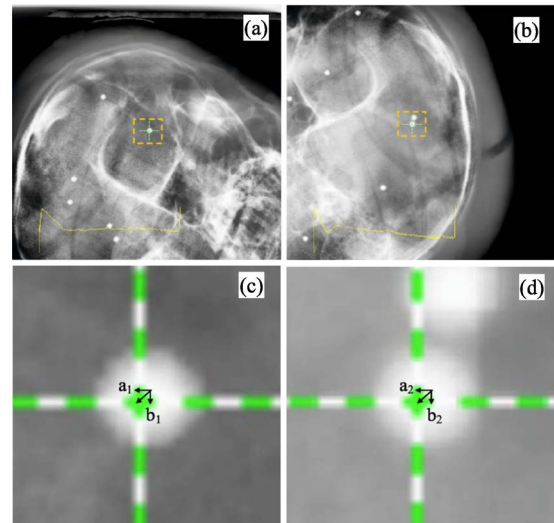


FIG. 2. Two verification x-ray images for evaluation of deviation between the x-ray isocenter (cross) and the planned isocenter (center of the BB). (a) Image 1, (b) Image 2, (c) amplification of the cross and the BB of Image 1, (d) amplification of the cross and the BB of Image 2.

evaluation of the image guidance system was conducted in such a phantom, while qualitative clinical reliability evaluation of the system was performed in patients.

### 1. Phantom study

Two tests were conducted for the phantom study. The first test was to statistically evaluate the localization accuracy of the image guided system with the isocenter at various locations of the skull. An anthropomorphic head phantom was implanted with eight 2-mm-diam metal spheres (BBs) at different locations (corresponding to right and left frontal lobes, right and left temporal lobes, right and left parietal lobes, occipital lobe and cerebellum) and attached with five infrared markers on the surface. CT images with 3 mm slice thickness were acquired and loaded into the BrainScan treatment planning system. An isocenter point was placed at the center of a BB, and the isocenter plan along with the CT images was sent to the ExacTrac/Novalis control computer. The phantom was first set up according to the external infrared markers. Then a random shift, which has both translational and rotational components, was induced to simulate possible patient setup errors using the mask system. The external markers were then removed, the reference star was attached to the couch, and the patient image guided localization procedure was followed. The image areas with implanted BBs were excluded for the “6D fusion.” After position readjustment, a pair of verification kV x-ray images were taken. Figures 2(a) and 2(b) show the two x-ray images. A cross representing the isocenter of the x-ray imaging system was overlapped with the BB of the planned isocenter. The accuracy of the localization for this isocenter was determined by evaluating the distance of the BB’s center to the cross center. Similarly, AP and lateral MV portal images were taken, and the accuracy of the localization of the planned isocenter to the linac’s isocenter was determined by

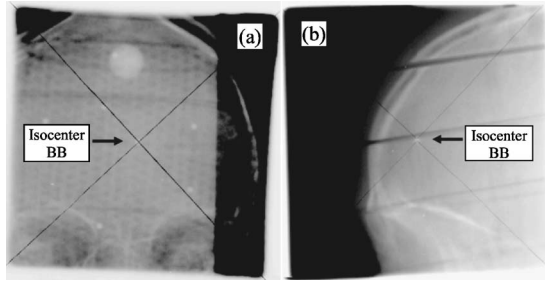


FIG. 3. Two MV portal films for evaluation of deviation between the linac isocenter (center of the irradiated portal) and the planned isocenter (center of the BB). (a) AP film, (b) lateral film.

the distance of the BB’s center to the linac’s isocenter, as shown in Fig. 3. The linac’s isocenter was defined by the two diagonals of the 9.8 cm × 9.8 cm square field. This process was repeated for each BB to obtain the statistical result. A correlation between the isocenters of the x-ray system and the linac system could also be established from the test.

The second test was to evaluate the localization accuracy of the system with various initial setup errors in the same isocenter. The phantom was setup with translation deviations ranging from -3 to 3 cm and rotational deviations ranging from -4 degrees to 4 degrees in a single direction or multiple directions. The 6D fusion image guided localization procedure was followed after each initial setup. Similarly, the isocenter BB’s position in the kV verification x-ray images after localization was used to determine the accuracy in translational directions. The “6D fusion” of the verification images was also performed and the difference of the rotational deviations from the localization images and the verification images was used to evaluate the capability of determining the rotational errors for the “6D fusion.” This test was repeated for two different BBs on different days.

Because the two x-ray projections are not in orthogonal directions to each other, nor in the horizontal plane, the measured deviation components in the x-ray imaging coordinate system (as shown in Fig. 1) would be different from that in the patient coordinate system. A transformation of the deviation components in the x-ray imaging system into the patient coordinate system (x, y, z) is given as follows:

$$x_2 = \frac{a_1 \cos \theta - a_2 \sin \theta}{\cos 2\theta}, \tag{1a}$$

$$y_2 = \frac{a_1 \sin \theta - a_2 \cos \theta}{\cos 2\theta}, \tag{1b}$$

$$z_2 = \frac{b_1 + b_2}{2} \tag{1c}$$

and

$$x = -\frac{\sqrt{2}}{2}x_2 \cos \gamma + \frac{\sqrt{2}}{2}y_2 \cos \gamma, \tag{2a}$$

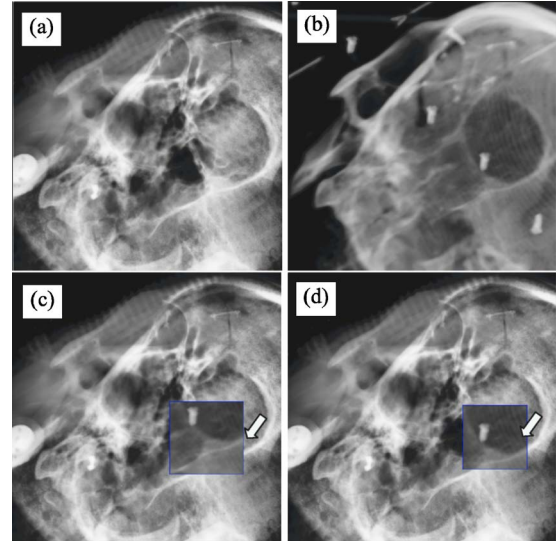


FIG. 4. Evaluation of the patient positioning accuracy by comparing the bony structure in the x-ray image with that in the corresponding DRR using the spy glass. (a) x-ray image, (b) corresponding DRR, (c) spy glass check of matching before 6D fusion, (d) spy glass check of matching after 6D fusion. The arrows in figures (c) and (d) show the difference of anatomic matching before and after fusion.

$$y = -\frac{\sqrt{2}}{2}x_2 \cos \gamma - \frac{\sqrt{2}}{2}y_2 \cos \gamma + z_2 \sin \beta, \tag{2b}$$

$$z = x_2 \sin \gamma + y_2 \sin \gamma + z_2 \cos \beta, \tag{2c}$$

where  $a_1, b_1$  and  $a_2, b_2$  are the isocenter deviations in two coordinate directions in image 1 image 2, respectively;  $x_2, y_2, z_2$  are the isocenter deviations in the Cartesian coordinate system  $X_2Y_2Z_2$ , which has its origin at the isocenter of the x-ray system,  $Z_2$  axis being perpendicular to the plane  $A_1B_1A_2B_2$ , and the middle line of the angle  $B_1OB_2$  also equally dividing the right angle formed by  $X_2, Y_2$  axis. In our system,  $\alpha=62^\circ, \theta=(90-\alpha)/2=14^\circ, \beta=53^\circ, \gamma=35^\circ$ .

**2. Patient study**

We evaluated the accuracy and reliability of the image-guided system in 12 consecutive patients with cranial lesions who underwent the image-guided FSRT procedure from January 2005 to July 2005. The study was approved by the Institutional Research Board. The number of fractions of treatment varied from 5 to 30 for each patient with a total of 127 fractions. Anatomic matches between DRRs and the kV x-ray images for each fraction, and between DRRs and the AP/lateral MV portal images for each patient were used for qualitative evaluation. Figures 4(a)–4(d) show an example of an x-ray image and the corresponding DRR, and the “spy glass” evaluation of their anatomic matches before and after 6D fusion. There was a significant mismatch between the x-ray image and the DRR before the “6D fusion” for this patient, as shown by the spy glass in Fig. 4(c). No such mismatch was observed after the fusion, as shown in Fig. 4(d). Figures 5(a) and 5(b) show an example of an AP portal film and the corresponding DRR for a patient. The portal

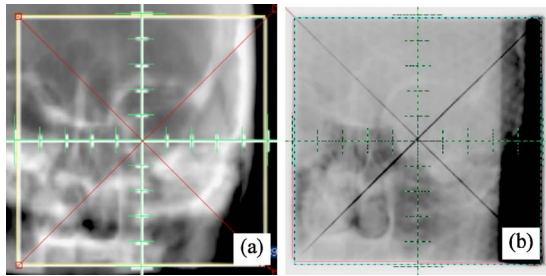


FIG. 5. Evaluation of the patient positioning accuracy by comparing the bony structures in the MV portal images and the corresponding DRR. (a) AP DRR, (b) AP portal image.

image was taken with  $9.8\text{ cm} \times 9.8\text{ cm}$  collimator opening (maximal opening in our system). The following specific parameters were considered in the qualitative evaluation: (1) the number of prominent anatomic landmarks in the images, (2) the maximal estimated anatomic mismatch between the DRRs and the images in any direction, and (3) the comparability of the anatomic matches to those in the phantom study.

### C. Using “6D fusion” as a gold standard

#### 1. Evaluation of the mask based stereotactic system

The “6D fusion” is an ideal tool to evaluate the accuracy of the mask based stereotactic system and other localization systems. The translational and rotational setup errors of the mask system at each fraction could be determined by the “6D fusion” results in the image guided localization procedure after a patient was set up with the mask system. The overall localization accuracy of the mask system was obtained by statistically analyzing these setup errors for all 127 fractions. In addition, the reproducibility of the mask system, which represents the variation between different fractions for a given patient, was also analyzed for all images from 127 fractions. The quantity “reproducibility” at a particular fraction of a patient was defined as the setup error subtracting the mean setup error for that patient.

#### 2. Evaluation of the “3D fusion” method

The “6D fusion” was also used as a gold standard to evaluate the accuracy of the “3D fusion” image guided method, which had been used for target localization for extracranial radiosurgery before the “6D fusion” was developed. For all kV images taken in 127 fractions, both “3D

fusion” and “6D fusion” were performed. The accuracy of 3D fusion was determined as the difference of the fusion results between the two methods. This translational difference was also compared with the rotational errors detected by the 6D fusion for each fraction.

### D. Statistic analysis

In this study, the position accuracy of a localization method was evaluated by another method as a gold standard with multiple measurements in various conditions. The mean ( $\bar{U}$ ) and the standard deviation ( $\sigma$ ) of the measurements were calculated and the result was expressed as  $\bar{U} \pm \sigma$ . The mean of a set of the measurements represents a systematic error of the method to be evaluated, or a systematic difference between the two methods if the gold standard had a systematic error itself. The reliability of the measured systematic error (i.e., the mean) can be represented by the standard error of mean (SEM), which is expressed as  $SEM = \sigma / \sqrt{N}$ , where  $N$  is the number of measurements. The standard deviation is a measure of random error, or the variation of the method. The 95% confidence interval (CI) was also used to represent the variation (random error) and the reliability of the systematic error (standard error of mean). If a localization method has a measured accuracy of  $\bar{U} \pm \sigma$ , then there is 95% confidence that the random position error falls in the range of  $[\bar{U} - 2\sigma, \bar{U} + 2\sigma]$ , and 95% confidence that there is a systematic error falling in the range of  $[\bar{U} - 2\sigma / \sqrt{N}, \bar{U} + 2\sigma / \sqrt{N}]$ .

## III. RESULTS

### A. Evaluation of the “6D fusion” system

#### 1. Phantom results

Table I shows the statistical results of the localization accuracy for eight different isocenters determined by both kV x-ray images and MV portal images in  $X$ ,  $Y$ , and  $Z$  directions in the patient coordinate system. The magnitude of the 3D vector displacement difference is also included. The difference between the two methods is calculated to determine the systematic difference between the isocenters of the kV x-ray and the linac systems. The results can be summarized as following: (1) The random error, which mainly represents the variations of the “6D-fusion” software to correctly register various images, and the ExacTrac system to correctly adjust the position, was less than 0.6 mm in terms of 95% CI in each direction. (2) There was a small but detectable system-

TABLE I. Statistic results of the target localization accuracy (mean values and standard deviations) of the “6D fusion” image guided system evaluated by kV x rays and MV portal films for eight planning isocenters in an anthropomorphic phantom.

	$X$ (mm)	$Y$ (mm)	$Z$ (mm)	3D vector
kV images	$-0.11 \pm 0.16$	$-0.37 \pm 0.29$	$-0.14 \pm 0.30$	$0.56 \pm 0.20$
MV portals	$-0.61 \pm 0.21$	$-0.14 \pm 0.22$	$-0.01 \pm 0.22$	$0.69 \pm 0.23$
Difference between kV and MV	$-0.49 \pm 0.14$	$0.22 \pm 0.16$	$-0.13 \pm 0.20$	$0.61 \pm 0.14$

TABLE II. Statistical results of the target localization accuracy and rotational variation of the “6D fusion” image guided system for various initial setup positions in two planning isocenters in an anthropomorphic phantom. The axis  $X$ ,  $Y$  and  $Z$  represent the lateral, longitudinal and PA directions. The angles  $\alpha$ ,  $\beta$  and  $\gamma$  represent the rotational angles around the  $X$ ,  $Y$ , and  $Z$  axis.

	Translational deviations (mm)				Rotational deviations (degree)		
	$X$	$Y$	$Z$	3D vector	$\alpha$	$\beta$	$\gamma$
Isocenter 1	$-0.01 \pm 0.13$	$-0.46 \pm 0.31$	$0.01 \pm 0.19$	$0.52 \pm 0.29$	$0.02 \pm 0.06$	$0.03 \pm 0.09$	$0.05 \pm 0.08$
Isocenter 2	$-0.08 \pm 0.20$	$-0.30 \pm 0.40$	$0.14 \pm 0.19$	$0.57 \pm 0.20$	$0.07 \pm 0.11$	$0.03 \pm 0.08$	$0.02 \pm 0.08$
Combining 1 and 2	$-0.04 \pm 0.16$	$-0.40 \pm 0.35$	$0.06 \pm 0.19$	$0.53 \pm 0.25$	$0.05 \pm 0.09$	$0.03 \pm 0.08$	$0.03 \pm 0.08$

atic error measured by the kV x-ray method, primarily in the longitudinal ( $Y$ ) direction, with the 95% CI of  $0.37 \pm 0.2$  mm. (3) There was also a systematic difference between the kV x-ray imaging and the MV portal imaging methods, mainly in the lateral ( $X$ ) direction, with a 95% CI of  $0.49 \pm 0.05$  mm.

Table II gives the results of the localization accuracy and angular variation for various initial setup positions for two different isocenters measured with the phantom on two different days, respectively. The results showed: (1) The systematic and random errors in the  $X$  and  $Z$  directions were remarkably smaller than that in the  $Y$  (longitudinal) direction for both isocenters. This indicates that the 3 mm slice thickness of the CT images influences the accuracy of the 2D/3D auto fusion in the longitudinal direction. (2) Overall, the systematic and random errors for two isocenters measured on two different days were consistent with each other, and also comparable to that obtained from various planning isocenter locations, as shown in Table I. (3) The angular variation was small, demonstrating that the translational shifts would not significantly change the rotational setting.

## 2. Patient data

Table III shows the summary of the results for the parameters used for the evaluations in patients. Bony structures that were clearly visualized on both the x-ray images and the DRRs were considered as anatomic landmarks. The mandible, which appeared sometimes in the images when the isocenter was in the inferior portion of the cranium and could have relative motion with the skull, was not considered as a reliable anatomic landmark. The number of anatomic landmarks was determined by the image with fewer landmarks in a pair of images for a fraction. The patient study showed: (1) Abundant anatomic landmarks were available for the kV images to evaluate the matches, mainly due to the oblique projection of the x rays to take the images. (2) The kV images

and the corresponding DRRs showed excellent anatomic matches in all 127 fractions. These matches were comparable to that in the cases of the phantom study. (3) The MV portal images and corresponding DRRs also showed reasonable anatomic matches. Although the mismatches were larger than that in the kV images, they were comparable or better compared to the corresponding mismatches between the MV portal images and DRRs in the phantom study. These results demonstrate that the “6D fusion” based image guided localization for patient setup is clinically reliable, and has similar localization accuracy to the phantom study.

## B. “6D fusion” to evaluate other methods

### 1. Evaluation of the mask based stereotactic system

Figures 6(a) and 6(b) show the plots of each measured position setup errors of the mask based localization system in the lateral versus longitudinal directions, and in the AP versus longitudinal directions for the 12 patients. The statistical summary of these position variations in three translational directions, as well as in three rotational directions, for each patient and for all patients overall, are listed in Table IV. In addition, the summary of the overall reproducibility, which was defined as the setup error subtracting the mean setup error of a patient, is also shown in Table IV.

The overall systematic errors in the lateral ( $X$ ) and longitudinal ( $Y$ ) directions were  $X = -0.37$  mm,  $Y = -0.29$  mm, respectively. These errors were negligible compared to the large random variations. However, a 0.93 mm systematic error in AP direction was noted. This systematic error was significant and true, considering that the standard error of mean (SEM) =  $\pm 0.09$  mm. This could be due to mask shrinkage or poor fitting of the posterior mask that resulted in systematically higher AP setup positions. Indeed, for several

TABLE III. Evaluation of the anatomic landmark matches for the kV x-ray images and MV images for 127 treatment fractions in 12 patients—summary of the number of pairs of images according to different evaluation parameters.

	Total pairs of images	Number of bony landmarks			Maximum mismatch in any directions			Compared to phantom study	
		1	2	>2	1 mm	1.5 mm	2 mm	Similar or better	Worse
KV x-ray images	127	0	0	127	127	0	0	127	0
MV portal images	12	1	2	9	5	6	1	12	0

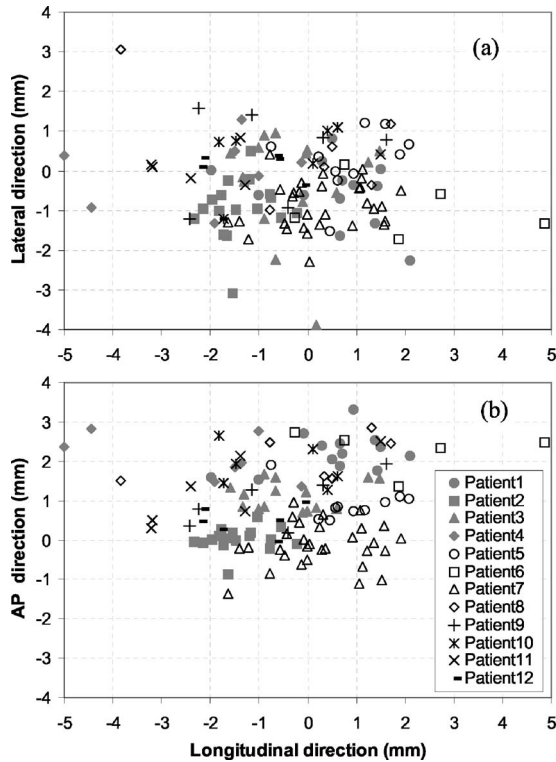


FIG. 6. Positioning differences between the mask system and the 6D fusion method for the total of 127 fractions in 12 patients. (a) Differences in lateral vs longitudinal directions, (b) differences in AP vs longitudinal directions.

of these patients, 1–4 mm spacers had to be added to fit the patient comfortably into the mask. All these patients showed relatively larger mean AP deviations. The overall random variations were  $\pm 1.0$  mm in AP and lateral directions, and  $\pm 1.5$  mm in longitudinal direction in terms of standard deviation, or  $\pm 2.0$  and  $\pm 3.0$  mm in terms of 95% confident

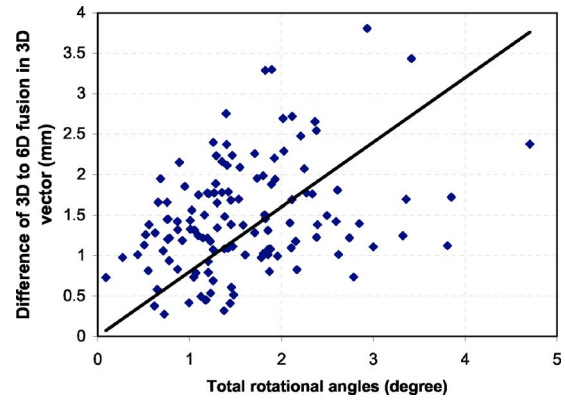


FIG. 7. The overall position difference between the 3D and 6D fusion methods vs the total rotational angle for 127 fractions.

intervals. The overall variation for the 3D vector was  $2.10 \pm 0.97$  mm in terms of the standard deviation.

The overall reproducibility was  $\pm 0.48$ ,  $\pm 0.84$ , and  $\pm 1.12$  mm in terms of the standard deviation in the AP, lateral and longitudinal directions, respectively. These were considerably smaller than the corresponding overall random variations, especially in the AP direction. This was understandable because the reproducibility did not account for the mask-to-mask or patient-to-patient variation. The day-to-day AP variation for a patient in the same mask is typically very small due to the nature of mask immobilization.

**2. Evaluation of the “3D fusion” method**

The overall position difference between the “3D fusion” and “6D fusion” was  $0.09 \pm 0.87$ ,  $0.51 \pm 0.87$ , and  $-0.19 \pm 0.88$  mm in terms of mean and standard deviations in the AP, lateral and longitudinal directions, respectively. The variations in the three orthogonal directions were almost the

TABLE IV. The position variations of the mask system in three translational directions and three rotational directions for each patient, and overall uncertainty and reproducibility for all patients measured by the 6D fusion method. The reproducibility was defined as the setup error subtracting the mean setup error of a patient.

Patients	Image sets	Translational axis (mm)				Rotational axis (degree)		
		AP	Sup/inf	Lateral	3D vector	AP	Sup/inf	R/L
Patient 1	10	0.92±0.41	0.88±0.85	0.26±0.79	1.64±0.62	-0.87±0.59	0.75±0.86	0.80±0.51
Patient 2 <sup>a</sup>	7	2.08±0.58	-2.2±1.8	0.00±0.88	3.30±1.55	-1.02±0.55	0.86±0.77	0.93±0.36
Patient 3 <sup>a</sup>	5	2.29±0.54	1.98±1.96	-0.92±0.73	3.55±1.21	-1.12±0.73	1.05±0.41	-0.70±0.71
Patient 4	30	-0.13±0.55	0.27±0.94	-0.89±0.60	1.46±0.51	0.53±0.66	0.80±0.54	-0.21±0.67
Patient 5 <sup>a</sup>	13	2.22±0.52	0.54±1.16	-0.54±0.76	2.68±0.56	0.11±0.33	-0.44±0.75	0.80±0.45
Patient 6	17	0.02±0.30	-1.4±0.59	-0.95±0.76	1.84±0.67	-0.56±0.41	0.31±0.22	0.22±0.25
Patient 7	15	1.13±0.36	-0.33±0.92	-0.30±1.32	1.86±0.78	-0.30±0.85	1.23±0.40	0.29±0.61
Patient 8 <sup>a</sup>	6	2.07±0.58	-0.12±2.01	0.60±1.43	2.95±1.26	-0.21±1.54	0.59±1.59	-0.4±1.76
Patient 9	6	0.99±0.67	-0.71±1.55	0.41±1.20	2.19±0.72	1.13±0.31	0.24±1.16	0.95±0.87
Patient 10 <sup>a</sup>	6	1.87±0.53	-0.65±1.14	0.43±0.86	2.41±0.55	0.16±0.46	0.66±0.31	3.03±1.07
Patient 11 <sup>a</sup>	6	1.25±0.90	-1.66±1.76	0.15±0.42	2.73±0.64	-0.58±1.06	0.89±1.41	0.79±0.35
Patient 12	6	0.49±0.36	-1.26±0.91	-0.08±0.62	1.57±0.76	-0.66±0.28	0.63±1.09	0.85±0.64
Overall uncertainty	127	0.93±1.03	-0.29±1.49	-0.37±0.99	2.10±0.97	-0.15±0.90	0.62±0.85	0.43±1.01
Reproducibility	127	0.0±0.48	0.0±0.84	0.0±1.12	0.0±1.45	0.0±0.66	0.0±0.72	0.0±0.66

<sup>a</sup>The patient had a spacer added to the mask during target localization and treatment.

TABLE V. Summary of the localization uncertainty for different techniques reported in the literature.

Authors	No. of patients (images)	Positioning technique	Positioning uncertainty (mm)				3D Vector (95% CI)	Evaluation technique
			AP	Lateral	Sup/inf			
This study	12 (127)	6D fusion	$<0\pm 0.48$	N/A <sup>a</sup>	N/A <sup>a</sup>	N/A <sup>a</sup>	AP reproducibility in mask	
Salter (Ref. 4)	8 phantom	6D fusion	$0.61\pm 0.21$	$0.14\pm 0.22$	$0.01\pm 0.22$	$1.05^b$	Phantom with implanted marker	
	9 (35)	TALON 1 <sup>st</sup> FX	$0.56\pm 0.30$	$0.52\pm 0.38$	$0.46\pm 0.25$	1.55	Anatomic land marks (points) in CT	
		Middle of treatment	$0.47\pm 0.33$	$0.73\pm 0.56$	$0.43\pm 0.27$	1.90		
Kumar (Ref. 21)	15 (123)	End of treatment	$0.61\pm 0.53$	$1.07\pm 0.50$	$0.63\pm 0.46$	2.47		
		GTC Frame	$-0.2\pm 1.0$	$0.7\pm 1.0$	$0.1\pm 1.2$	3.4	Bony structure match in portal images	
Karger (Ref. 17)	4 (118/52) <sup>c</sup>	Mask	$1.22\pm 0.25$	$0.35\pm 0.41$	$0.74\pm 0.32$	3.0	Implanted markers in x-ray portal images	
Hamilton (Ref. 18)	12 (104)	Mask	$0.0\pm 1.1$	$0.0\pm 1.0$	$0.0\pm 1.4$	$\approx 4.0$	Embedded markers in mouth piece, portal film	
Willner (Ref. 16)	16 (22)	Mask	$0.1\pm 1.2$	$-0.1\pm 1.8$	$0.4\pm 1.5$	5.0	Target, anatomic structure in CT	
This study	12 (127)	Mask	$0.93\pm 1.03$	$-0.37\pm 0.99$	$-0.29\pm 1.49$	4.0	6D fusion, x-ray images	
		Mask reproducibility	$0.0\pm 0.48$	$0.0\pm 0.84$	$0.0\pm 1.12$	2.9		

<sup>a</sup>N/A: Not Available.

<sup>b</sup>Include the isocenter uncertainty caused by gantry rotation.

<sup>c</sup>118 image sets for a total of 52 fractions of treatment. Only one image set was used for evaluation for each fraction for the rest of the methods.

same. Figure 7 shows these differences in the 3D vector versus the total rotational angle for the 127 fractions. The total rotational angle was calculated as the square root of the sum of the square for each rotational angle. The difference between the 3D and 6D fusion methods was less than 2.5 mm for 119/127 (94%) fractions. However, there were four fractions for which the difference was larger than 3.0 mm. The fractions with such large differences tended to also have relatively large total rotational angles, suggesting a relationship with the total rotational angle.

#### IV. DISCUSSION

We have developed a clinical procedure using the 2D/3D image fusion guided target localization system for fractionated cranial stereotactic radiotherapy. The phantom study (Table I) demonstrated that the maximal random error of using this image guided system for target localization was  $\pm 0.6$  mm in terms of the 95% CI in any individual coordinate direction. A small systematic error was also detected, and varied slightly with the methods of kV x-ray or MV portal images. The systematic error for kV x-ray method was approximately 0.4 mm, primarily in the longitudinal direction, possibly due to the uncertainty of determining the BB's center in the CT images with 3 mm slice thickness. A 0.5 mm systematic difference between the isocenters of the kV x-ray

and the linac system, mainly in the lateral direction, was also detected. Two factors contributed to this systematic difference: (1) The uncertainty of calibrating the x-ray system isocenter to the linac isocenter defined by the room laser system with laser linewidth of about 1 mm. (2) The difference of the linac isocenter defined by the room laser system and the linac isocenter defined by the AP and right lateral portal films. It should be pointed out that the measured random and systematic errors represent the accuracy and the precision of positioning the patient isocenter point to an ideal linac isocenter defined by the room Laser system. In actual treatments, the overall treatment related positioning error should also include the linac isocenter position variation due to gantry and couch rotations.

Although the Novalis system uses an oblique x-ray configuration, the phantom study results demonstrated that the sophisticated "6D fusion" software was able to accurately register two x-ray images of the rigid phantom with its CT simulation images. However, an accurate image fusion software alone was not enough to guarantee an accurate image-guided localization system. The infrared based ExacTrac system also contributed to the accurate target localization. The treatment couch position readout usually had a resolution of 1 mm and an uncertainty of about 2 mm. In addition, the three couch motion directions might not always be consistent



with the three Cartesian coordinator directions defined in the image fusion software, especially due to couch sagging. With the help of a reference star attached to the table, the control of the couch position can be transferred to the ExacTrac system, and the couch position can be adjusted to the correct isocenter position with a high degree of accuracy.

The human head is a relatively rigid object with rich bony structures. A cooperative patient usually does not move his head during treatment when he is immobilized by the head mask. Therefore, the image guided system should theoretically achieve similar localization accuracy in patients as in the phantom, because the accuracy of image fusion is mainly determined by the extension of image deformation between two image sets to be fused together. Evaluation of the anatomic matches between the kV x-ray images and DRRs, and between MV portal images and DRRs showed that the localization accuracy in patients was comparable to the phantom study. The “6D fusion” has also been used to evaluate the overall position accuracy and reproducibility of the head mask system. The results could be used to test the accuracy of both the object (the head mask system) and the evaluation method (image fusion). The measured variation should be the combination of the true variation of the object and the uncertainty of the measurement method. Our results showed that the measured reproducibility of the mask in the AP direction was  $\pm 0.48$  mm in terms of standard deviation, which corresponds to  $\pm 0.96$  mm in terms of 95% CI. This demonstrated that the “6D fusion,” as a measurement method, had an accuracy better than  $\pm 0.96$  mm in 95% CI in the AP direction for patients. This is another perspective to partially support that accurate image fusions were achieved in these patients.

The thermal plastic mask has been widely used for immobilization of cranial patients in radiotherapy. Many studies have been published to evaluate the position uncertainty for this immobilization method.<sup>16–18</sup> However, the results vary largely, mainly because there was no suitable evaluation method available, and different numbers of patients/image sets were used for evaluation. The “6D fusion” provides an ideal tool to evaluate the position uncertainty for the mask immobilization system. It provides both accurate translational and rotational errors. In this study, by evaluating a number of patients with multiple fractions, we were also able to distinguish the overall uncertainty from the reproducibility of the mask system. Table V compares the position uncertainty of the mask immobilization system reported by some of the studies in the literature,<sup>16–18</sup> along with the results of this study. In addition, the position uncertainties of some other localization methods for FSRT are also listed in this table for comparison.<sup>4,21</sup> The 95% CI for the position uncertainty for the mask system was 3.0, 4.0, and 5.0 mm by Karger *et al.*,<sup>19</sup> Hamilton *et al.*,<sup>20</sup> and Willner *et al.*,<sup>18</sup> respectively, compared to the 4.0 mm overall uncertainty, and 2.9 mm reproducibility in this study.

The 6D fusion method also measured the rotational deviation for each patient initially set up with the mask system. The measured rotational angles with the AP axis, longitudinal axis and lateral axis were  $-0.1 \pm 0.9$ ,  $0.6 \pm 0.9$  and

$0.4 \pm 1.0$  degrees, respectively. This was consistent with the results reported by Hamilton *et al.*,<sup>20</sup> which were  $\pm 0.9$ ,  $\pm 0.9$  and  $\pm 0.8$  degrees, respectively. This indicates that the 95% CI of the rotational deviation was about  $1.8^\circ$  in each direction. As mentioned, the “6D fusion” image guided localization system did not correct the rotational errors at this time. This  $1.8^\circ$  angular deviation would have a minimal effect on target coverage for small target volumes. We estimated that a  $2^\circ$  angular deviation would induce a positional deviation of about 1 mm at the block edge 3 cm away from the isocenter. However, for large targets with rotational deviations larger than  $2^\circ$ , the positional deviation induced at the block edge would be significant. A 6D adjustable treatment table that corrects for the rotational errors will be installed in our system in the near future to minimize such rotational deviation induced errors. A rotational deviation could also induce considerable errors for the simple “3D fusion” to adjust the isocenter position, as demonstrated in Fig. 6, and for position evaluations using portal films, because the prominent bony structures used for fusion or evaluation could be far away from the isocenter.

## V. CONCLUSION

The phantom and patient studies demonstrated that the 2D/3D image fusion guided localization system is an accurate and reliable target localization method for FSRT of cranial lesions. The 2D/3D fusion is also an ideal tool to evaluate the localization accuracy of the mask based stereotactic system. Using 2D/3D image fusion greatly improves the position accuracy compared to the mask based localization system.

<sup>a)</sup> Author to whom correspondence should be addressed. Electronic mail: [jjin1@hfhhs.org](mailto:jjin1@hfhhs.org)

<sup>1</sup>S. E. Combs, D. Schulz-Ertner, D. Moschos, C. Thilmann, P. E. Huber, and J. Debus, “Fractionated stereotactic radiotherapy of optic pathway gliomas: Tolerance and long-term outcome,” *Int. J. Radiat. Oncol., Biol., Phys.* **62**(3), 814–819 (2005).

<sup>2</sup>R. C. Torres, L. Frighetto, A. A. De Salles, B. Goss, P. Medin, T. Solberg, J. M. Ford, and M. Selch, “Radiosurgery and stereotactic radiotherapy for intracranial meningiomas,” *Neurosurg. Focus* **14**(5), e5 (2003).

<sup>3</sup>D. C. Shrieve, L. Hazard, K. Boucher, and R. L. Jensen, “Dose fractionation in stereotactic radiotherapy for parasellar meningiomas: Radiobiological considerations of efficacy and optic nerve tolerance,” *J. Neurosurg.* **101**(Suppl. 3), 390–395 (2004).

<sup>4</sup>B. J. Salter, M. Fuss, D. G. Vollmer, A. Sadeghi, C. A. Bogaev, D. A. Cheek, T. S. Herman, and J. M. Hevezi, “The TALON removable head frame system for stereotactic radiosurgery/radiotherapy: Measurement of the repositioning accuracy,” *Int. J. Radiat. Oncol., Biol., Phys.* **51**(2), 555–562 (2001).

<sup>5</sup>R. J. Bale, M. Voegelé, W. Freysinger, A. R. Gunkel, A. Martin, K. Bumm, and W. F. Thumfart, “Minimally invasive head holder to improve the performance of frameless stereotactic surgery,” *Laryngoscope* **107**(3), 373–377 (1997).

<sup>6</sup>S. S. Gill, D. G. T. Thomas, A. P. Warrington, and M. Brada, “Relocatable frame for stereotactic external beam radiotherapy,” *Int. J. Radiat. Oncol., Biol., Phys.* **20**, 599–603 (1991).

<sup>7</sup>M. Dellannes, N. Daly-Schweitzer, J. Sabatuer, and J. Bonnet, “Fractionated brain stereotactic irradiation using a non-invasive frame: Technique and preliminary results,” *Radiat. Oncol. Invest.* **2**, 92–98 (1994).

<sup>8</sup>M. I. Hariz, R. Henriksson, P. O. Lofroth, L. V. Laitinen, and N. E. Saterberg, “A non-invasive method for fractionated stereotactic irradiation of brain tumors with linear accelerator,” *Radiother. Oncol.* **17**, 57–72 (1990).

- <sup>9</sup>J. S. Tsai, M. J. Engler, M. N. Ling, J. K. Wu, B. Kramer, T. Dipetrillo, and D. E. Wazer, "A non-invasive immobilization system and related quality assurance for dynamic intensity modulated radiation therapy of intracranial and head and neck disease," *Int. J. Radiat. Oncol., Biol., Phys.* **43**(2), 455–467 (1999).
- <sup>10</sup>A. F. Thornton, R. K. Ten Haken, A. Gerhardtsson, and M. Correll, "Three-dimensional motion analysis of an improved head immobilization system for simulation CT, MRI, and PET imaging," *Radiother. Oncol.* **20**, 224–228 (1991).
- <sup>11</sup>B. D. Milliken, S. J. Rubin, R. J. Hamilton, L. S. Johnson, and G. T. Chen, "Performance of a video-image-subtraction-based patient positioning system," *Int. J. Radiat. Oncol., Biol., Phys.* **38**(4), 855–866 (1997).
- <sup>12</sup>S. L. Meeks, F. J. Bova, W. A. Friedman, J. M. Buatti, R. D. Moore, and W. M. Mendenhall, "IRLED-based patient localization for linac radiosurgery," *Int. J. Radiat. Oncol., Biol., Phys.* **41**(2), 433–439 (1998).
- <sup>13</sup>K. P. Gall, L. J. Verhey, and M. Wagner, "Computer assisted positioning of radiotherapy patients using implanted radiopaque fiducials," *Med. Phys.* **20**, 1153–1159 (1993).
- <sup>14</sup>M. J. Murphy, "An automatic six-degree-of-freedom image registration algorithm for image-guided frameless stereotaxic radiosurgery," *Med. Phys.* **24**, 857–866 (1997).
- <sup>15</sup>B. G. Baumert, P. Egli, S. Studer, C. Dehing, and J. B. Davis, "Repositioning accuracy of fractionated stereotactic irradiation: Assessment of isocentre alignment for different dental fixations by using sequential CT scanning," *Radiother. Oncol.* **74**(1), 61–66 (2005).
- <sup>16</sup>J. Willner, M. Flentje, and K. Bratengeier, "CT simulation in stereotactic brain radiotherapy-analysis of isocenter reproducibility with mask fixation," *Radiother. Oncol.* **45**(1), 83–88 (1997).
- <sup>17</sup>C. P. Karger, O. Jakel, J. Debus, S. Kuhn, and G. H. Hartmann, "Three-dimensional accuracy and interfractional reproducibility of patient fixation and positioning using a stereotactic head mask system," *Int. J. Radiat. Oncol., Biol., Phys.* **49**(5), 1493–1504 (2001).
- <sup>18</sup>R. J. Hamilton, F. T. Kuchnir, C. A. Pelizzari, P. J. Sweeney, and S. J. Rubin, "Repositioning accuracy of a noninvasive head fixation system for stereotactic radiotherapy," *Med. Phys.* **23**(11), 1909–1917 (1996).
- <sup>19</sup>J. Y. Jin, S. Ryu, J. Rock, K. Faber, M. Gates, S. Li, and B. Movsas, "Image-guided target localization for stereotactic radiosurgery: Accuracy of 6D versus 3D image fusion," *Radiosurgery* **6**, 50–59 (2006).
- <sup>20</sup>L. T. Wang *et al.*, "Infrared patient positioning for stereotactic radiosurgery of extracranial tumors," *Weld. Int.* **31**, 101–111 (2001).
- <sup>21</sup>S. Kumar, K. Burke, C. Nalder, P. Jarrett, C. Mubata, R. A'hern, M. Humphreys, M. Bidmead, and M. Brada, "Treatment accuracy of fractionated stereotactic radiotherapy," *Radiother. Oncol.* **74**(1), 53–59 (2005).